Letter | Editors' Suggestion

How roughness and thermal properties of a solid substrate determine the Leidenfrost temperature: Experiments and a model

Yuki Wakata,[1] Ning Zhu,[1] Xiaoliang Chen,[1] Sijia Lyu,[1] Detlef Lohse,[2,3,*] Xing Chao,[1,†] and Chao Sun[1,4,‡]

[1]*Center for Combustion Energy, Key Laboratory for Thermal Science and Power Engineering of Ministry of Education, Department of Energy and Power Engineering, Tsinghua University, 100084 Beijing, China*

[2]*Physics of Fluids Group, MESA+ Institute and J. M. Burgers Centre for Fluid Dynamics, University of Twente, P.O. Box 217, 7500AE Enschede, The Netherlands*

[3]*Max Planck Institute for Dynamics and Self-Organization, 37077 Göttingen, Germany*

[4]*Department of Engineering Mechanics, School of Aerospace Engineering, Tsinghua University, Beijing 100084, China*

(Received 9 August 2022; revised 23 February 2023; accepted 24 May 2023; published 8 June 2023)

In this Letter, we systematically investigate the Leidenfrost temperature for hot solid substrates with various thermal diffusivities and surface roughnesses. Based on the experimental results, we build a phenomenological model that considers the thermal diffusivity of a solid substrate and derive a relationship between the surface roughness and the resulting vapor film thickness. The generality of this model is supported by experimental data for different liquids and solid substrates. Our model thus allows for a theoretical prediction of the Leidenfrost temperature and develops a comprehensive understanding of the Leidenfrost effect.

DOI: 10.1103/PhysRevFluids.8.L061601

Drops normally boil when deposited on surfaces with temperature above the boiling point of the liquid. However, when the surface temperature exceeds the Leidenfrost temperature T_L, a vapor layer generated by the evaporation levitates the drop, preventing contact and reducing the heat transfer between the drop and the surface [1,2]. This effect, known as the Leidenfrost effect, has received much attention in recent years, both for its beauty and the rich physics involved in it [3–5] and for its various practical applications [6–11]. Therefore, learning and regulating the transition temperature T_L is of scientific and practical value.

It has been observed that the Leidenfrost temperature T_L of a static liquid drop on a flat surface is affected by several factors, including the properties of the solid surface (thermal properties, surface roughness, surface structure [12–15]), the ambient condition (pressure and temperature [16,17]), and the properties of the liquid [18], including the contact angle on the substrate [19,20]. Although theoretical models have been developed for T_L in terms of film stability [21–25], the common approaches often assume that the substrate is isothermal or of uniform temperature, which is at odds with the finding that surfaces can be cooled by the floating Leidenfrost drop, as quantitatively shown in Ref. [26]. However, the influence of the thermal properties of the solid on T_L has not yet been systematically studied.

*d.lohse@utwente.nl
†chaox6@tsinghua.edu.cn
‡chaosun@tsinghua.edu.cn

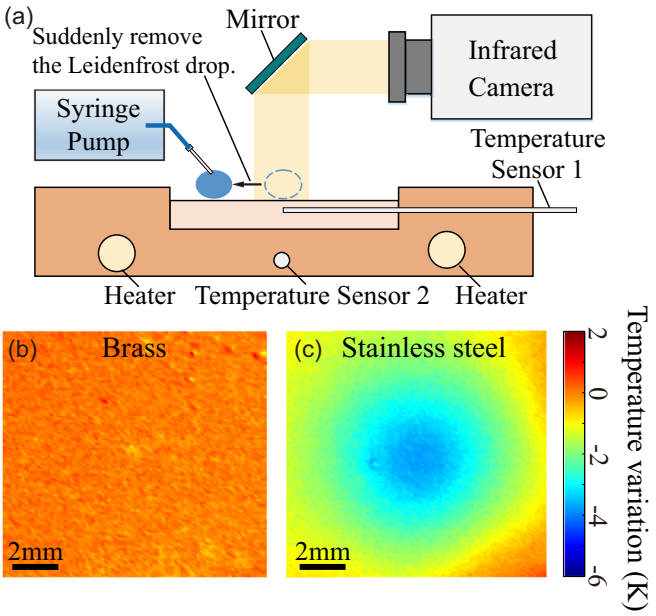

FIG. 1. The cooling effect of a Leidenfrost drop. (a) Schematic of the experimental setup. A water drop is placed on a smooth plate and fixed by a feeding needle for a while. Then the drop is suddenly moved away, and a high-speed infrared camera is used to measure the instantaneous temperature field of the surface. Surface temperature variation of brass (b) and stainless steel (c) surfaces compared to the initial temperature field after the Leidenfrost drop (drop radius $\approx$2 mm) has evaporated for 60 s.

In this Letter, we show how the thermal properties and surface roughness of a solid substrate affect the Leidenfrost effect and the Leidenfrost temperature T_L. The surface cooling caused by a Leidenfrost drop is shown with the help of infrared imaging, and Leidenfrost temperatures of water and ethanol drops on various surfaces are obtained with the aim to understand the dependence on the solid thermal diffusivity α and the surface roughness S_a. A theoretical model describing the surface cooling effect is established and the influence of thermal properties on the vapor film thickness is obtained. Based on these findings, we propose a universal law with which we can predict T_L for different liquid drops on substrates with different thermal properties and surface roughness.

To capture the surface cooling effect caused by a Leidenfrost drop, we place a water drop on a heated substrate with an initial surface temperature $T_{s0} = 240\ ^\circ$C, which is well above the Leidenfrost temperature, and use a 14-gauge metal needle to control the movement of the drop [see Fig. 1(a)]. The drop evaporates at a fixed location for 60 s, then it is removed with the help of the needle within 0.05 s, exposing the surface underneath (see Movie S1 [27]). A high-speed infrared camera (Telops FAST L200) immediately records the temperature field of the solid surface. The surface temperature recovery during the fast removal process is proved to be less than 0.8 K (see the Supplemental Material [27] for details of the temperature recovery). With the initial homogeneous and known surface temperature, the cooling caused by the drop evaporation can thus be quantitatively characterized.

Figures 1(b) and 1(c) compare the temperature reduction of brass and stainless steel surfaces after having a water droplet thereon for 60 s. The initial surface temperature is 296 $^\circ$C and the drop radius $\approx$2 mm. The stainless steel surface has a maximum temperature reduction of 6 K, while the temperature of the brass surface remains almost unchanged [see Fig. 1(b)]. The plate temperature reduction due to the evaporation of the levitating Leidenfrost drop was also measured in Ref. [26] using an interferometry technique. Let us focus on the difference in the thermal diffusivity α of

TABLE I. Thermal diffusivity of the selected materials.

Property	Unit	Aluminum (Al)	Brass (Br)	1045 Carbon steel (CS)	Stainless steel (SS)
Thermal diffusivity α	m^2/s	0.907×10^{-4}	0.356×10^{-4}	0.136×10^{-4}	0.045×10^{-4}

these two materials listed in Table I. $\alpha = k_s/\rho_s c_s$ determines how quickly a material recovers from temperature variations, where k_s, ρ_s, c_s are thermal conductivity, density, and specific heat capacity of the solid, respectively. It is found that α of stainless steel is about 8 times smaller than brass, which may lead to the difference in surface temperature reduction during the Leidenfrost process.

The demonstrated surface temperature reduction will subsequently affect the vapor generation and thus the stability of the Leidenfrost stage. To study this dependence, we measure the lifetime τ of a sessile droplet with a fixed volume $V_0 = 30.6$ μl as a function of the initial surface temperature T_{s0} to determine the Leidenfrost temperature [1]. Details of the experimental setup are given in the Supplemental Material [27]. Four candidate materials with decreasing thermal diffusivity α—aluminum, brass, carbon steel (Type 1045), and stainless steel (Type 304)—are selected as substrates. An exemplary surface local surface profile obtained by a 3D interference profiler (ZYGO Nexview) is shown in Fig. 2(a). The surface roughness S_a is defined as the average surface height deviations from the mean line. In our experiments, S_a varies from 0.1 to 2.8 μm, which is much larger than what typical smooth surfaces have, $S_a \approx 0.02$ μm [12].

Figure 2(b) shows the lifetime τ of a water droplet versus the initial surface temperature T_{s0} on substrates of different materials but with a similar roughness ($S_a = 0.6 \sim 1.0$ μm). The Leidenfrost temperature T_L is defined by the specific initial surface temperature T_{s0} that relates to the maximum

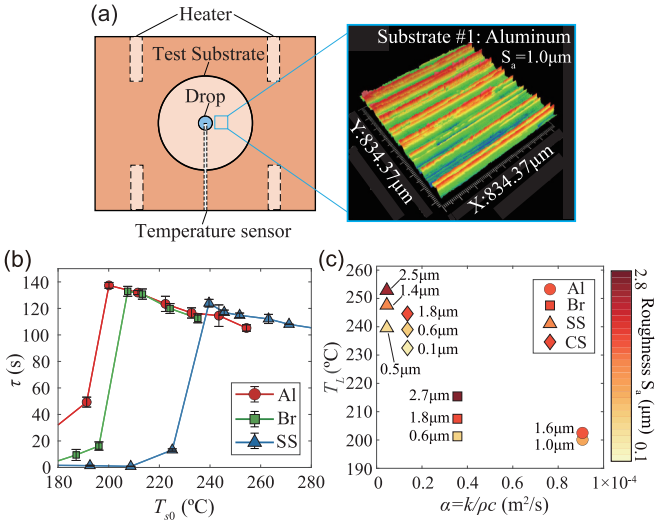

FIG. 2. Measuring the Leidenfrost temperature T_L. (a) Top view of the experimental setup. A test substrate is placed on the heating base with four heating rods. A temperature sensor is placed at a depth of 2 mm from the surface of the test substrate. The inset shows the 3D surface roughness profile of part of a test substrate (aluminum, $S_a = 1.0$ μm) obtained by an interference profiler (ZYGO Nexview). (b) Measured lifetime of a water drop ($V_0 = 30.6$ μl) on aluminum (Al), brass (Br), and stainless steel (SS) substrates. (c) The Leidenfrost temperature T_L as a function of thermal diffusivity α and surface roughness S_a. The color of the symbols represents the value of S_a. The exact values of S_a are labeled beside the symbols.

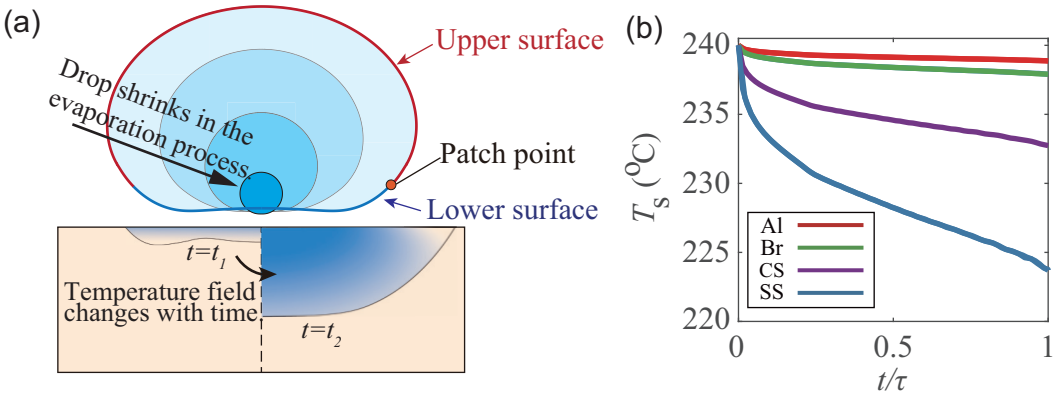

FIG. 3. (a) The evaporation process of a Leidenfrost drop on a solid substrate. Darker drop colors represent later times. (b) Temporal variation of the surface temperature T_s with initial value $T_{s0} = 240\ ^\circ$C. T_s is calculated as the average surface temperature directly below the drop.

lifetime τ of a drop on a superheated surface [18,28]. It is shown that T_L of the droplet on brass is lower than T_L on stainless steel, while higher than T_L on aluminum, which is exactly opposite to the trend of their thermal diffusivity (see Table I). Extending our experiments to surfaces with different roughness, the so-determined Leidenfrost temperatures are plotted as a function of the thermal diffusivity α and the surface roughness S_a in Fig. 2(c). It can be seen that T_L increases with increasing surface roughness for fixed material and decreases with increasing thermal diffusivity for fixed roughness.

For a more quantitative explanation of the experimental observations, we develop a simple theoretical model that simulates the evaporation process of a Leidenfrost droplet from a certain volume till its final fate [see Fig. 3(a)]. The temperature variation of the substrate during the evaporation process is considered, while the internal flow and the temperature gradient in the drop are neglected. The evaporation process of the drop is assumed to be quasistatic.

In the model the drop geometry is divided into upper and lower regions by the patch point following Ref. [29] [see Fig. 3(a)]. While the shape of the upper drop surface is determined by a balance between the hydrostatic pressure and the surface tension, the geometry of the lower surface is obtained from the thin film equation for the vapor layer within the lubrication approximation, assuming axial symmetry [25,26,29]. The variation of the temperature profile of the solid substrate $T(r, z)$ during the evaporation process is numerically calculated using the transient heat diffusion equation $\frac{1}{\alpha}\frac{\partial T}{\partial t} = \frac{\partial}{\partial r}(r\frac{\partial T}{\partial r}) + \frac{\partial^2 T}{\partial z^2}$. The solid surface is divided into two regions according to the projected area of the lower drop surface. The cooling heat flux $q(r)$ is assumed to only affect the region right beneath the lower droplet surface, while an adiabatic boundary condition is used for the outer region. A detailed description of this model can be found in the Supplemental Material [27].

We calculate the evaporation process of a Leidenfrost drop with the initial volume of $V_0 = 30.6$ μl till a very small volume of $V_{end} = 0.4$ μl, which is close to the size of a Leidenfrost drop approaching its final fate [30,31]. Through the calculation, we quantitatively obtain the cooling effect of a Leidenfrost droplet on different surfaces [see Fig. 3(b)]. For materials with high α such as aluminum and brass, the surface temperature reduction is less than 2 K, while for stainless steel with much smaller α (see Table I) the maximum temperature reduction is near 20 K.

Concurrent with the surface cooling, the weaker evaporation flux reduces the vapor pressure in the film, resulting in lower vapor film thickness [26]. Figure 4(a) illustrates the variation of the minimum thickness of the vapor film, δ_{min}, on substrates with $T_{s0} = 240\ ^\circ$C of various materials, including an ideal surface ($\alpha \to \infty$). It can be seen that with decreasing α for realistic materials, the minimum film thickness δ_{min} deviates further from the ideal result. The difference is quite small

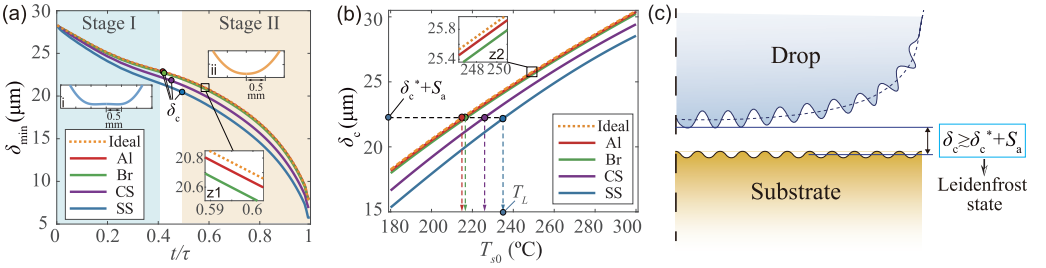

FIG. 4. (a) Minimum film thickness δ_{min} vs normalized time t/τ on surfaces of different materials with initial temperature $T_{s0} = 240$ °C. Inset (z1) shows a local zoom of the results to better differentiate the upper three curves. The two stages of the variation of δ_{min} are marked using different colors. The bottom geometries of the two stages are shown in inset (i) and inset (ii), which show the bottom surface with and without a dimple shape, respectively. The transition points related to δ_c of each curve are marked by solid symbols. (b) Characteristic film thickness δ_c as a function of the initial surface temperature T_{s0} on aluminum (Al), brass (Br), carbon steel (CS), stainless steel (SS), and ideal surfaces. Inset (z2) shows a local zoom. (c) A schematic diagram showing the fluctuation profile of the liquid-vapor interface and the solid surface.

for aluminum and brass surfaces due to their relatively high thermal diffusivities while much larger for carbon steel and stainless steel surfaces. This trend holds for all initial surface temperatures T_{s0}.

The temporal variation of δ_{min} in Fig. 4(a) can be divided into two stages according to the lower surface geometry of the drop. With the evaporation process, the bottom surface loses its dimple shape and the minimum position of the film thickness moves to the center, indicating the transition from the first stage to the second stage. The minimum film thickness at the transition moment is defined as the characteristic film thickness δ_c. In the second stage, the spatial and temporal fluctuations of the liquid-vapor interface are suppressed because now the surface tension takes the dominance in defining the geometry [32], resulting in more stable levitation of the Leidenfrost drop until its final fate. Therefore, δ_c represents the minimum film thickness before the stable period in the Leidenfrost drop evaporation process. Figure 4(b) shows that δ_c increases with initial temperature T_{s0} and thermal diffusivity α of the substrate.

As an inherently unstable system, the Leidenfrost drop is known to suffer from various instabilities [3,22–24,33–35], which induce fluctuations with an amplitude on the order of 5 μm at the liquid-vapor interface [32]. The fluctuation, combined with the roughness of the solid surface, results in significant inhomogeneity of the local vapor thickness δ [see Fig. 4(c)]. Under the influence of the wavy geometry of both the drop and the solid surface, the associated overpressure of the vapor layer ΔP experiences strong variation [32], which causes further fluctuation of the liquid-gas interface. As the characteristic film thickness δ_c becomes smaller, the undulated liquid interface is more likely to penetrate the vapor film and directly contact the heated surface [1,3]. Direct contact leads to strong nucleate boiling of the drop and further increase of the contact area [3,35,36], bringing the Leidenfrost stage to an end [37].

To prevent such collapse of the vapor film and to maintain the Leidenfrost state, the characteristic film thickness δ_c must be larger than a critical value. For a perfectly smooth surface, this critical value is defined as δ_c^*, which relates only to the liquid properties. For surfaces with finite roughness, the film thickness must be increased to compensate for the effect of roughness. Here we propose the criterion $\delta_c \gtrsim \delta_c^* + S_a$, which considers a simple linear effect of the roughness on the critical film thickness required to maintain the Leidenfrost stage and is consistent with the view of the Leidenfrost transition as a directed percolation process [3].

Using the criterion $\delta_c \gtrsim \delta_c^* + S_a$, we can explain how thermal diffusivity and surface roughness affect the Leidenfrost temperature T_L. As the surface roughness S_a increases, a thicker vapor film is required to maintain the Leidenfrost state. Since the characteristic film thickness δ_c monotonically increases with the initial surface temperature T_{s0}, the increment of S_a leads to a higher T_L,

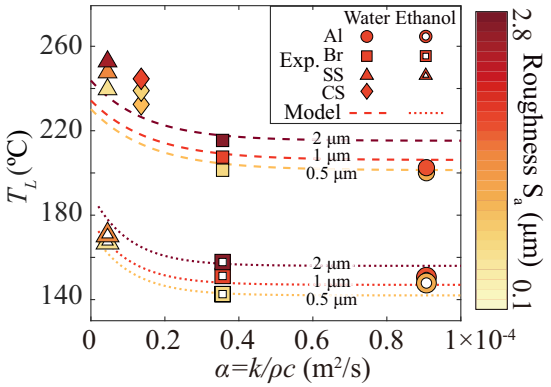

FIG. 5. T_L resulting from our model for water (dashed line) and ethanol drops (dotted line) on surfaces with different roughness ($S_a = 2, 1, 0.5$ μm), compared to experimentally measured values of water (solid markers) and ethanol drops (hollow markers). The colors of the markers correspond to the value of the surface roughness S_a, which is also given for the curves.

as evidenced by the above experiments. The effects of the thermal diffusivity α on T_L can be understood through $\delta_c(T_{s0})$ dependencies that refer to different thermal diffusivities in Fig. 4(b). For poorly diffusive materials such as stainless steel, the decline in surface temperature reduces the characteristic vapor layer thickness δ_c, and a higher initial surface temperature is required for sufficient film thickness to meet the stability criterion. As a result, the T_L decreases with increasing thermal diffusivity α. However, for materials with relatively high α like aluminum and brass, the cooling effect is negligible, and further increases in α have little effect on T_L.

To obtain the T_L for surfaces of different materials and surface roughness, we interpolate the value of $\delta_c^* + S_a$ into the $\delta_c(T_{s0})$ dependencies to get the transition temperature [see the illustration in Fig. 4(b)]. Here we choose three typical values of surface roughness ($S_a = 0.5, 1, 2$ μm) to show a basic trend of the effect of roughness. The exact value of δ_c^* can be approximated by experimentally measuring the Leidenfrost temperature T_L on an extremely low roughness surface and interpolating the obtained T_L into the $\delta_c(T_{s0})$ dependency.

The obtained T_L values are fitted with the function $y = ae^{bx+c} + d$ and plotted in Fig. 5 as dashed lines, together with the experimental results. The experimental and model results are also shown for ethanol droplets to illustrate the generality of our model. As can be seen, our simple model shows good agreement with the experimental data. Moreover, the model predicts that T_L decreases with increasing α for the same liquid and gradually converges to a nearly constant temperature, as we have already speculated.

In summary, we showed by infrared thermometry the nonnegligible cooling effects of Leidenfrost drops on surfaces with small thermal diffusivities. The influence of thermal properties and surface roughness on the Leidenfrost temperature was then investigated experimentally and explained by a simple theoretical model. We proposed the criterion $\delta_c \gtrsim \delta_c^* + S_a$ based on the stability of the vapor film in Leidenfrost stage. Combining the model and the experimental results, we showed that this model can be extended to different fluids and solid substrates. In future work, the present model should be extended to the dynamic Leidenfrost effect [37] by considering the impact process of the droplet to help to predict and control the Leidenfrost temperature in practical applications.

The data that support the findings of this study are available from the corresponding author upon reasonable request.

This work was supported by National Natural Science Foundation of China under Grants No. 11988102, 91852202, 51976105, and 91841302, the New Cornerstone Science Foundation through

the XPLORER prize, ERC Advanced Grant DDD, Project No. 740479, and NWO through the Multiscale Catalytic Energy Conversion (MCEC) Research Center.

[1] A.-L. Biance, C. Clanet, and D. Quéré, Leidenfrost drops, Phys. Fluids **15**, 1632 (2003).
[2] D. Quéré, Leidenfrost dynamics, Annu. Rev. Fluid Mech. **45**, 197 (2013).
[3] P. Chantelot and D. Lohse, Leidenfrost Effect as a Directed Percolation Phase Transition, Phys. Rev. Lett. **127**, 124502 (2021).
[4] A. Bouillant, C. Cohen, C. Clanet, and D. Quéré, Self-excitation of Leidenfrost drops and consequences on their stability, Proc. Natl. Acad. Sci. USA **118**, e2021691118 (2021).
[5] S. Lyu, H. Tan, Y. Wakata, X. Yang, C. K. Law, D. Lohse, and C. Sun, On explosive boiling of a multicomponent Leidenfrost drop, Proc. Natl. Acad. Sci. USA **118**, e2016107118 (2021).
[6] J. Kim, Spray cooling heat transfer: The state of the art, Int. J. Heat Fluid Flow **28**, 753 (2007).
[7] G. Liang and I. Mudawar, Review of spray cooling—Part 2: High temperature boiling regimes and quenching applications, Int. J. Heat Mass Transf. **115**, 1206 (2017).
[8] I. U. Vakarelski, J. D. Berry, D. Y. Chan, and S. T. Thoroddsen, Leidenfrost Vapor Layers Reduce Drag without the Crisis in High Viscosity Liquids, Phys. Rev. Lett. **117**, 114503 (2016).
[9] A. Gauthier, C. Diddens, R. Proville, D. Lohse, and D. van der Meer, Self-propulsion of inverse Leidenfrost drops on a cryogenic bath, Proc. Natl. Acad. Sci. USA **116**, 1174 (2019).
[10] A. Bouillant, T. Mouterde, P. Bourrianne, A. Lagarde, C. Clanet, and D. Quéré, Leidenfrost wheels, Nat. Phys. **14**, 1188 (2018).
[11] R. Abdelaziz, D. Disci-Zayed, M. K. Hedayati, J.-H. Pöhls, A. U. Zillohu, B. Erkartal, V. S. K. Chakravadhanula, V. Duppel, L. Kienle, and M. Elbahri, Green chemistry and nanofabrication in a levitated Leidenfrost drop, Nat. Commun. **4**, 2400 (2013).
[12] N. Nagai and S. Nishio, Leidenfrost temperature on an extremely smooth surface, Exp. Therm. Fluid Sci. **12**, 373 (1996).
[13] H. Kim, B. Truong, J. Buongiorno, and L.-W. Hu, On the effect of surface roughness height, wettability, and nanoporosity on Leidenfrost phenomena, Appl. Phys. Lett. **98**, 083121 (2011).
[14] M. Jiang, Y. Wang, F. Liu, H. Du, Y. Li, H. Zhang, S. To, S. Wang, C. Pan, J. Yu *et al.*, Inhibiting the Leidenfrost effect above 1, 000 °C for sustained thermal cooling, Nature (London) **601**, 568 (2022).
[15] R. Wu, O. Lamini, and C. Zhao, Leidenfrost temperature: Surface thermal diffusivity and effusivity effect, Int. J. Heat Mass Transf. **168**, 120892 (2021).
[16] F. Celestini, T. Frisch, and Y. Pomeau, Room temperature water Leidenfrost droplets, Soft Matter **9**, 9535 (2013).
[17] M. A. van Limbeek, O. Ramírez-Soto, A. Prosperetti, and D. Lohse, How ambient conditions affect the Leidenfrost temperature, Soft Matter **17**, 3207 (2021).
[18] K. J. Baumeister and F. F. Simon, Leidenfrost temperature: Its correlation for liquid metals, cryogens, hydrocarbons, and water, J. Heat Transf. **95**, 166 (1973).
[19] P. Bourrianne, C. Lv, and D. Quéré, The cold Leidenfrost regime, Sci. Adv. **5**, eaaw0304 (2019).
[20] D. Panchanathan, P. Bourrianne, P. Nicollier, A. Chottratanapituk, K. K. Varanasi, and G. H. McKinley, Levitation of fizzy drops, Sci. Adv. **7**, eabf0888 (2021).
[21] J. D. Bernardin and I. Mudawar, The leidenfrost point: Experimental study and assessment of existing models, J. Heat Transf. **121**, 894 (1999).
[22] C. H. Panzarella, S. H. Davis, and S. G. Bankoff, Nonlinear dynamics in horizontal film boiling, J. Fluid Mech. **402**, 163 (2000).
[23] E. Aursand, S. H. Davis, and T. Ytrehus, Thermocapillary instability as a mechanism for film boiling collapse, J. Fluid Mech. **852**, 283 (2018).
[24] T. Y. Zhao and N. A. Patankar, The thermo-wetting instability driving Leidenfrost film collapse, Proc. Natl. Acad. Sci. USA **117**, 13321 (2020).

[25] C. Cai, I. Mudawar, H. Liu, and C. Si, Theoretical Leidenfrost point (LFP) model for sessile droplet, Int. J. Heat Mass Transf. **146**, 118802 (2020).

[26] M. A. van Limbeek, M. H. K. Schaarsberg, B. Sobac, A. Rednikov, C. Sun, P. Colinet, and D. Lohse, Leidenfrost drops cooling surfaces: Theory and interferometric measurement, J. Fluid Mech. **827**, 614 (2017).

[27] See Supplemental Material at http://link.aps.org/supplemental/10.1103/PhysRevFluids.8.L061601 for the experimental setup and methods for measuring the Leidenfrost temperature and the surface cooling, details of the theoretical model and calculation methods, film thickness of small Leidenfrost drops, and the calculation of the temperature variation during the infrared experiment.

[28] B. Gottfried, C. Lee, and K. Bell, The Leidenfrost phenomenon: Film boiling of liquid droplets on a flat plate, Int. J. Heat Mass Transf. **9**, 1167 (1966).

[29] B. Sobac, A. Rednikov, S. Dorbolo, and P. Colinet, Leidenfrost effect: Accurate drop shape modeling and refined scaling laws, Phys. Rev. E **90**, 053011 (2014).

[30] F. Celestini, T. Frisch, and Y. Pomeau, Take Off of Small Leidenfrost Droplets, Phys. Rev. Lett. **109**, 034501 (2012).

[31] S. Lyu, V. Mathai, Y. Wang, B. Sobac, P. Colinet, D. Lohse, and C. Sun, Final fate of a Leidenfrost droplet: Explosion or takeoff, Sci. Adv. **5**, eaav8081 (2019).

[32] G. Graeber, K. Regulagadda, P. Hodel, C. Küttel, D. Landolf, T. M. Schutzius, and D. Poulikakos, Leidenfrost droplet trampolining, Nat. Commun. **12**, 1727 (2021).

[33] G. I. Taylor, The instability of liquid surfaces when accelerated in a direction perpendicular to their planes. I, Proc. R. Soc. London A **201**, 192 (1950).

[34] V. P. Carey, *Liquid-Vapor Phase-Change Phenomena: An Introduction to the Thermophysics of Vaporization and Condensation Processes in Heat Transfer Equipment*, 3rd ed. (CRC Press, Boca Raton, FL, 2020).

[35] P. Chantelot and D. Lohse, Drop impact on superheated surfaces: Short-time dynamics and transition to contact, J. Fluid Mech. **928**, A36 (2021).

[36] D. Harvey, J. M. Harper, and J. C. Burton, Minimum Leidenfrost Temperature on Smooth Surfaces, Phys. Rev. Lett. **127**, 104501 (2021).

[37] T. Tran, H. J. J. Staat, A. Prosperetti, C. Sun, and D. Lohse, Drop Impact on Superheated Surfaces, Phys. Rev. Lett. **108**, 036101 (2012).